ELSEVIER

Applied Mathematical Modelling 23 (1999) 881–897

APPLIED MATHEMATICAL MODELLING

www.elsevier.nl/locate/apm

Two-phase modeling of batch sedimentation

M. Latsa [a], D. Assimacopoulos [a,*], A. Stamou [b], N. Markatos [a]

[a] *Department of Chemical Engineering, National Technical University of Athens, 9 Heroon Polytechniou, Zografou University Campus, 157 80 Zografou, Athens, Greece*

[b] *Department of Civil Engineering, National Technical University of Athens, 9 Heroon Polytechniou, Zografou University Campus, 157 80 Zografou, Athens, Greece*

Received 4 April 1997; received in revised form 15 January 1999; accepted 4 March 1999

Abstract

A two-phase model for the simulation of sedimentation processes is presented. The model solves the continuity and momentum equations for the pure-clear liquid and the sludge phases, and it is verified against a well-known benchmark problem, for which analytical solutions exist. Numerical simulations of a typical 1-D batch sedimentation process for mono-dispersed particles are carried out and results are found to be in satisfactory agreement with experimental data and model predictions of other researchers. A further expansion of the model to two-dimensions leads to predictions of the dynamic behavior of settling tanks and the effect of the inclination angle on the sedimentation process. © 1999 Elsevier Science Inc. All rights reserved.

Keywords: Two-phase flow; Batch sedimentation; Numerical modeling; Inclined settlers

1. Introduction

A wide variety of industrial separation technologies, such as clarification and thickening, employ sedimentation processes in order to remove solid particles from liquid streams and to thicken the sludge, that is formed. Typical batch sedimentation tests are used, in order to assess the susceptibility of a suspension to a full-scale separation installation.

During batch sedimentation, a suspension of particles is allowed to stand in a settling tank (or column). Usually, the tank is vertical to correspond to the traditional vertical settling tanks used in muchmany industrial applications. Settling of particles occurs through the action of gravity, leading to the formation of distinct settling layers and a sludge layer. The dynamic behavior of the sediment (settling and compressibility capacity) is portrayed by the thickness and composition changes of these layers.

Batch sedimentation was the subject of many research studies but most of them have been restricted to vertical settling tanks and to 1-D processes. Settling velocities were estimated by the standard or a modified Stokes equation and particle interactions by empirical relationships. Kynch [1], in his classical theory on batch sedimentation for mono-dispersed particles, introduced

* Corresponding author. Tel.: +30 1 7723218; fax: +30 1 7723155; e-mail: assim@chemeng.ntua.gr

PII: S0307-904X(99)00016-5

the particle conservation equation, in order to determine the sludge-liquid interface. Tiller [2] and Auzerais et al. [3] proposed modifications and extensions to Kynch's theory mainly for the particle conservation equation. They focused on the mechanism of the interactions between particles, such as particle inertial effect, inter-particle forces and sludge compressibility. Auzerais et al. [3] examined the effect of sludge compressibility, on the basis of various assumptions regarding the nature and mechanics of the compression. They also argued that for stable dispersion of small particles, the inter-particle force is equivalent to the osmotic pressure and they added a second-order (dispersion) term in the particle conservation equation.

Stamatakis and Tien [4] presented a model for the predictingon of the sludge-liquid interfacebatch sedimentation. Four years later Stamatakis and Tien [5] extended their model for compressible sludges and included. The extended model is based on the solution of the continuity equation for both the particle and fluid phases. They used Darcy's law for the description of the relative fluid/particle motion in the sludge region and empirical constitutive expressions relating the sludge's permeability and porosity with the compressible stress. The model incorporates existing correlations for estimating the settling velocity of the particles derived by the Stokes law.

The Stokes law in its standard or modified version has been used also in research studies concerning inclined settling tanks. Inclined settling tanks are frequently used in sedimentation processes because they accelerate the sedimentation process and are suitable for continuous processes. Davis et al. [6] presented a theoretical model for the sedimentation of polydisperse suspensions in inclined settlers. The settling velocity of the particles was estimated by a modified Stokes equation multiplied by a hindrance factor, while the concentration of solids was calculated by the continuity equation. Wang and Davis [7] solved numerically the continuity equations of solids and liquid, using a modified Stokes equation for the prediction of the velocity coalescing drops.

Bailey et al. [8] assumed different phases for the characteristic particle sizes and solved the momentum and continuity equations for each 'solid' phase. The velocity of the liquid phase was calculated by the volume balance equation. The compressibility of the sediment was estimated by the volume occupied by the solid particles in each time step. When a certain concentration of solid particles was reached (maximum packing of the sediment), it was assumed that no movement of liquid or solid could occur at this region.

Hanumanth et al. [9] modeled the sedimentation problem by solving the momentum and continuity equations for the solid phase. The velocity of the liquid phase was related to the velocity of a solid through a volumetric flux balance and the volume fraction of the liquid was considered to be the one satisfying the overall continuity equation. The compressibility of the sediment was not taken into account. Experimental work was also done in order to confirm the model predictions.

In the present study a general model is formulated for the description of the 1-D or 2-D sedimentation processes in vertical or inclined settling tanks. The model employs the continuity and momentum equations for the two-phase flow (liquid and sludge). The only empirical information needed by the model is the friction between the two phases and the final solids' concentration of the sludge. The settling velocities of the suspension are derived by the solution of the momentum equations. In contrast to Bailey's model, the present approach does not assume a continuous solid phase but a sludge phase (a mixture of clear liquid and solids), which is dispersed in the clear liquid. Information for the mean particle diameter, the densities of the solids and of the clear liquid and the maximum solids' concentration at the end of the process needs to be given. Bailey's model needs much more information for the sludge phase than the present one, which is not easily available. A comparison with Hanumanth' s model shows that the present model

follows a more rigorous formulation because it takes into account the sediment compressibility, through the assumption of a sludge phase, and through the use of the mixture viscosity in the interface friction correlation.

In the following sections the model is initially verified against a well-known benchmark problem (1-D batch sedimentation of a dilute suspension) and its predictions are compared to the analytical solution. The model is then expanded to the 1-D batch sedimentation process of monodispersed particles and verified against model predictions [5] and experimental data [9]. A final expansion of the model to two dimensions is demonstrated by simulating a 2-D settling tank with inclined walls. The two velocity components and the volume fraction profiles are calculated and they disclose the time history of the sedimentation process, as well as the effects of the inclination angle on the settling velocity of the particles.

2. The numerical model

2.1. Description of the problem

The system to be simulated is a rectangular tank of height L and length W (Fig. 1) which initially contains a uniform mixture of clear liquid and solids and is either vertical or inclined. During the sedimentation process, zones of different concentrations in solid are formed. The most significant ones are the zone of the clear liquid and the zone of the sludge, which increase in size, until a steady state is achieved.

The model assumes two phases. The first phase is the pure liquid and the second phase (sludge phase) is a mixture of solids and liquid. The concentration of the second phase in solids is the maximum solids' concentration that can be achieved (r_{smax}) during the sedimentation process.

The main assumptions used for the present model are the following:

- The interface force depends only on the friction between the solid particles and the liquid.
- The two phases are insoluble to each other. The main advantage of this assumption is that the maximum packing of the sediment can be defined and therefore a special handling of the sediment compressibility is not needed.
- Hindered settling is described by the interface friction force, which depends on the mean particle diameter and the solids' concentration.

2.2. Governing equations of the model

It is assumed that both phases coexist in time (t) and space (x, y). Any small volume in the flow domain contains at any time a volume fraction, r_i of each phase. The sum of the volume fractions of the two phases is always equal to unity, i.e.

$$r_1 + r_2 = 1, \tag{1}$$

where index 1 stands for the sludge and 2 for the pure liquid phase.

Each phase is treated as a continuum in the flow domain and the following governing equations can be derived for a 2-D sedimentation process [10].

Continuity:

$$\frac{\partial}{\partial t}(r_i\rho_i) + \frac{\partial}{\partial x}(r_i u_i \rho_i) + \frac{\partial}{\partial y}(r_i v_i \rho_i) = 0. \tag{2}$$

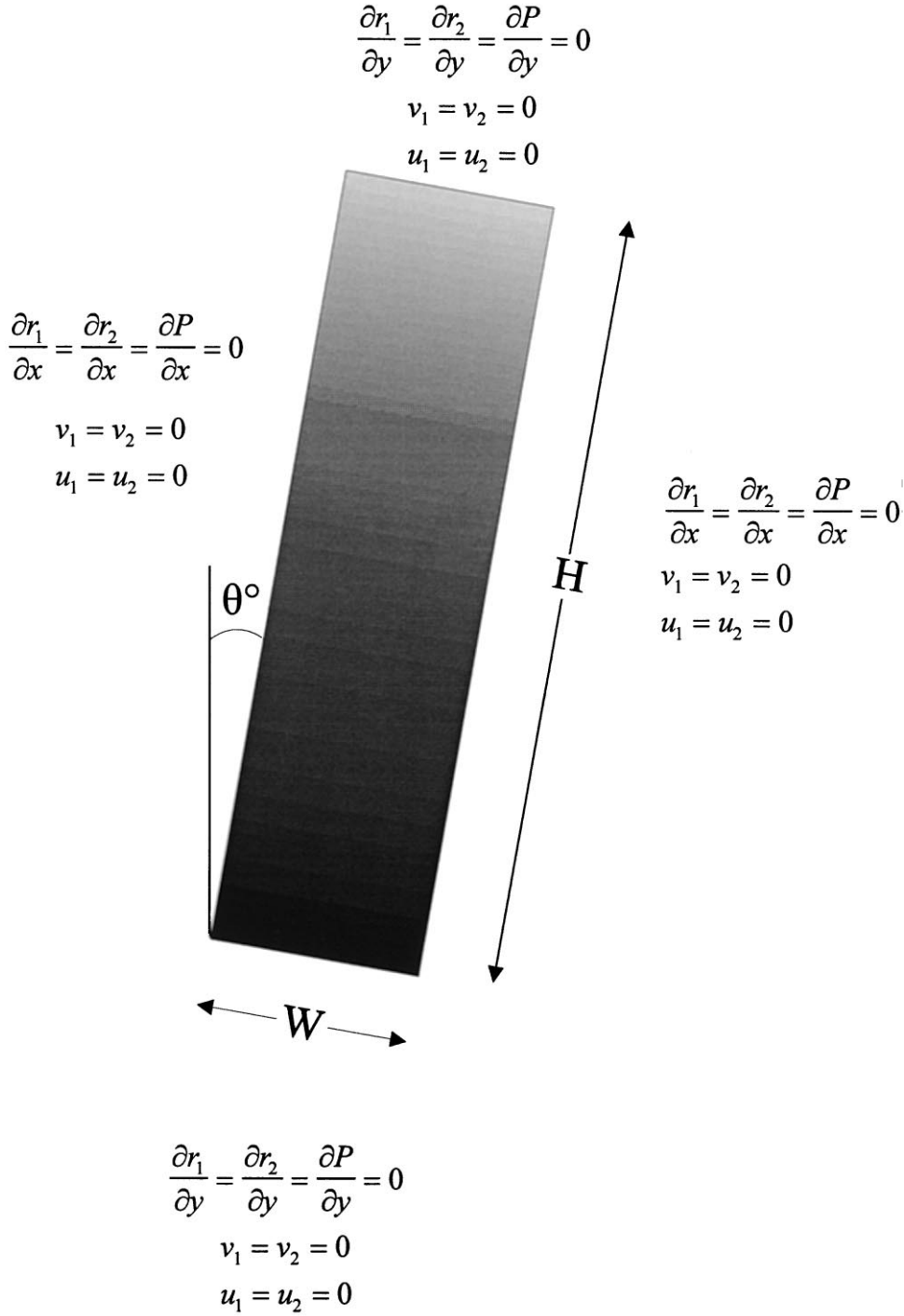

Fig. 1. Geometry and boundary conditions.

x-momentum:

$$\frac{\partial}{\partial t}(r_i\rho_i u_i)+\frac{\partial}{\partial x}(r_i\rho_i u_i u_i)+\frac{\partial}{\partial y}(r_i\rho_i v_i u_i)-\frac{\partial}{\partial x}\left(\mu_i\frac{\partial(r_i u_i)}{\partial x}\right)-\frac{\partial}{\partial y}\left(\mu_i\frac{\partial(r_i u_i)}{\partial y}\right)$$
$$=-r_i\frac{\partial P}{\partial x}-r_i\rho_i g_x+C_{ij}(u_j-u_i). \tag{3}$$

y-momentum:

$$\frac{\partial}{\partial t}(r_i\rho_i u_i)+\frac{\partial}{\partial x}(r_i\rho_i u_i v_i)+\frac{\partial}{\partial y}(r_i\rho_i v_i v_i)-\frac{\partial}{\partial x}\left(\mu_i\frac{\partial(r_i v_i)}{\partial x}\right)-\frac{\partial}{\partial y}\left(\mu_i\frac{\partial(r_i v_i)}{\partial y}\right)$$
$$=-r_i\frac{\partial P}{\partial y}-r_i\rho_i g_y+C_{ij}(v_j-v_i). \tag{4}$$

For each phase i, u_i is the velocity parallel to the direction x, v_i is the velocity parallel to the direction y, ρ_i is the density, μ_i is the viscosity, P is the pressure and g_x and g_y are the accelerations of gravity in the directions x and y, respectively.

The diffusion term

$$-\frac{\partial}{\partial x}\left(\mu_i\frac{\partial(r_i u_i)}{\partial x}\right)$$

in Eq. (3) can be expanded to:

$$-\frac{\partial}{\partial x}\left(\mu_i\frac{\partial(r_i u_i)}{\partial x}\right)=-\frac{\partial}{\partial x}\left(r_i\mu_i\frac{\partial(u_i)}{\partial x}\right)-\frac{\partial}{\partial x}\left(u_i\mu_i\frac{\partial(r_i)}{\partial x}\right),$$

where the first term of the right part represents a Fickian type diffusion, and the second term describes the phase diffusion, or as stated by others [16] the shear-induced diffusion due to concentration gradient.

The terms $C_{ij}(u_j-u_i)$ and $C_{ij}(v_j-v_i)$ in Eq. (3), represent the friction between the two phases, which depends strongly on the type of the system under consideration. For the benchmark problem, the interphase friction factor, C_{ij} can be approximated by the following relationship [13]:

$$C_{ij}=C_{\mathrm{f}}r_i r_j\bar{\rho}, \tag{5}$$

where $\bar{\rho}=r_1\rho_1+r_2\rho_2$ and C_{f} is the magnitude of the interphase friction. For suspensions of mono-dispersed solid particles of diameter d_{p}, the following equation [12] can be used:

$$C_{ij}=\frac{3}{4}\frac{C_{\mathrm{D}}r_{\mathrm{s}}\rho_{\mathrm{l}}}{d_{\mathrm{p}}}|u_{\mathrm{s}}-u_{\mathrm{l}}|. \tag{6}$$

C_{D} is the drag coefficient, which is a function of the particle Reynolds number, Re:

$$C_{\mathrm{D}}=\frac{24}{Re}(1+0.1Re^{0.75}), \tag{7}$$

$$Re=\frac{|u_{\mathrm{s}}-u_{\mathrm{l}}|d_{\mathrm{p}}\rho_{\mathrm{l}}}{\mu_{\mathrm{m}}}, \tag{8a}$$

where μ_{m} is the mixture viscosity, ρ_{l} is the density of the liquid and r_{s} is the volume fraction of solids ($\mathrm{m}^3_{\mathrm{solids}}/\mathrm{m}^3_{\mathrm{mixture}}$). The mixture and the sludge viscosities are calculated by the correlation proposed by Ishii and Zuber [12]:

$$\mu_{\mathrm{m}}=\mu_{\mathrm{f}}\left(1-\frac{r_{\mathrm{s}}}{r_{\mathrm{s(max)}}}\right)^{-2.5r_{\mathrm{s(max)}}}. \tag{8b}$$

The geometry and the boundary conditions, in the general case of an inclined settling tank, are illustrated in Fig. 1.

2.3. Derivation of the finite volume equations

Eqs. (2)–(4) are integrated over finite control volumes. A staggered grid is employed in the calculations [14], so that each velocity grid node lies between two scalar volumes. The volume fractions of each phase are calculated on the scalar nodes.

2.4. Solution procedure

An iterative solution procedure is used to solve the finite volume equations. The procedure is based on the Inter-Phase Slip Algorithm, IPSA [10], with an upwind differencing scheme.

2.5. The code

The computer code, TFLOW-2D, a modified version of the TEACH code, was used in the present study. TFLOW-2D was developed at the Computational Fluid Dynamics Section of the Department of Chemical Engineering at the National Technical University of Athens for solving two-phase two-dimensional problems, of plane or axisymmetric systems, involving parabolic or elliptic flows, with or without heat transfer.

3. Application of the model – results and discussion

3.1. 1-D batch sedimentation test

Initially, the model has been applied and verified in a simple, batch sedimentation test case in the 1-D settling tank (Depth, $H = 2.0$ m) of Fig. 2. At time $t = 0$, a dense liquid (ρ_1) rests at the

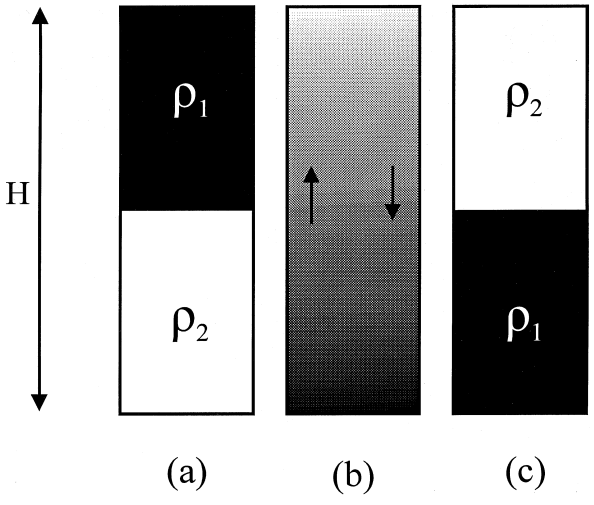

Fig. 2. The sedimentation test case.

upper half part ($r_1 = 1.0$) of the settling tank, above an equivalent volume ($r_2 = 1.0$) of a lighter liquid (ρ_2). Flow in the tank is 1-D with gravitational force acting downwards. As time proceeds, the lighter liquid rises to the top of the column, whilst the dense liquid sinks to the bottom (Fig. 2(b)). Eventually, all of the dense liquid will rest on the bottom of the column and the light liquid at the top (Fig. 2(c)). It has been observed [15] that the solution exhibits acute discontinuities, a fact that makes numerical predictions difficult.

Simulations of the transient behavior of the settling process are compared against analytical results and PHOENICS' [11] numerical results presented by Markatos [15]. The analytical solution can be obtained, only when density differences are small and the value of interphase friction is high enough; and furthermore, it is necessary:

(i) to neglect the acceleration terms in the momentum equations and;

(ii) to adopt the drift flux approximation [13].

The analytical solution is given in Appendix A.

In the present simulation, ρ_1 and ρ_2 are chosen equal to 1.0 and 0.999 kg/m^3, respectively. Eq. (5) is used for the calculation of the interphase friction factor and C_f is set equal to 1000. A computational grid consisting of 82 cells has been used, while the time step was set equal to 1 s. These values are identical to those used by Markatos [15].

The change of the predicted volume fractions of the dense liquid (r_1) with depth (y) for various times (t) is shown in Fig. 3 together with the computations of Markatos [15] and the analytical

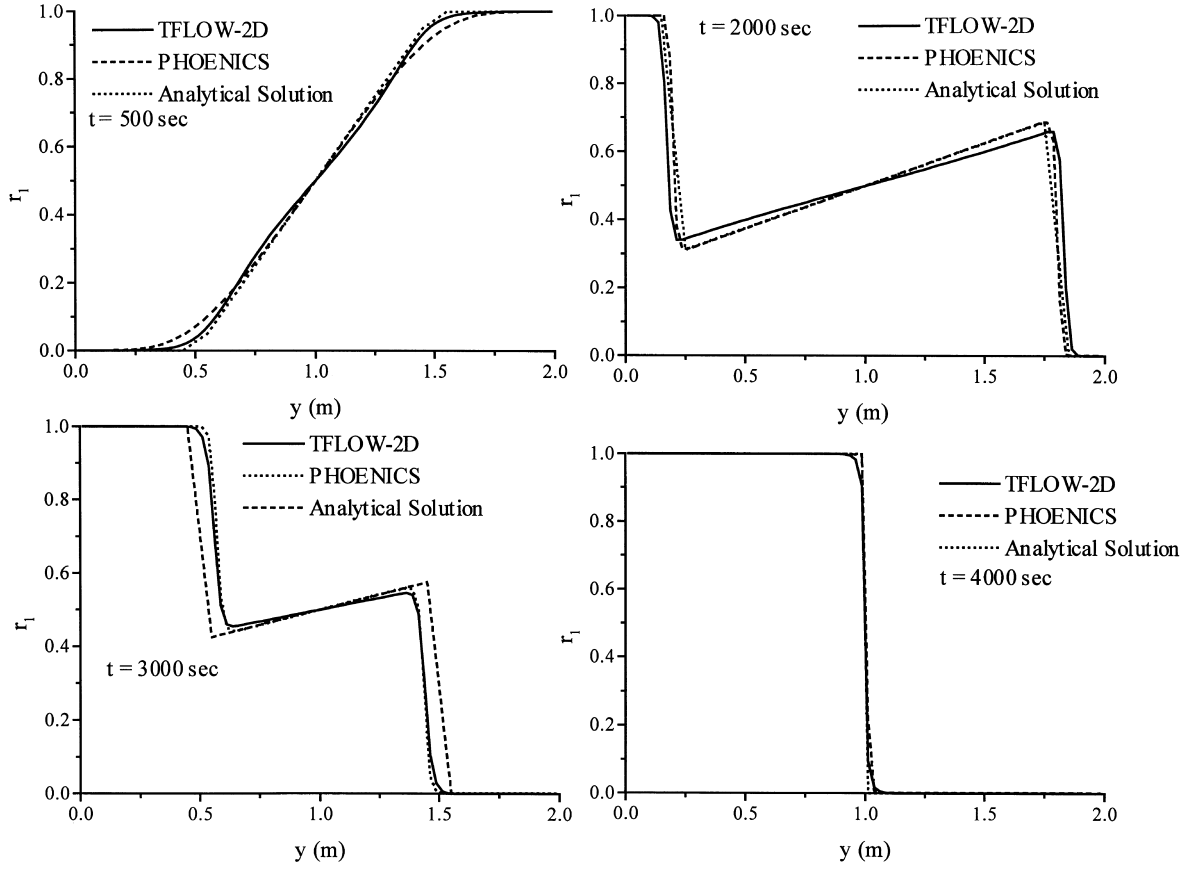

Fig. 3. Variation of r_1 with height (Y) and time (t).

solution. The results of the present model are in better agreement with the analytical solution and the wave-propagation speed is well predicted at all times, t. Overturning of the two liquids is completed at $t = 4000$ s. The small discrepancy from the analytical solution, which is observed near the relatively steep gradients of the r_1–y curve, can be attributed to the numerical diffusion of the low order discretization scheme.

3.2. 1-D batch sedimentation of mono-dispersed particles with sludge thickening

A suspension of monodispersed particles of diameter ($d_p = 75$ μm) and initial volume fraction ($r_S = 0.2$ m^3_{solid}/m^3_{mixt}) is allowed to stand in a tank of depth, $H = 1.0$ m and width, $W = 0.3$ m. The density of the particles ($\rho_s = 2500$ kg/m^3) is greater than the density of the liquid ($\rho_l = 1000$ kg/m^3) and they settle towards the bottom of the tank forming a sludge layer. The sludge layer increases with time, but as it becomes thicker, it is compressed (thickening process) until it reaches a constant height. During settling, three distinct layers are formed:

(i) the clear liquid layer at the top of the tank;
(ii) the sludge layer and;
(iii) the suspension layer, which has the same concentration in solids with the initial uniform suspension.

The suspension layer diminishes with time, while the other two layers increase.

The change over time of the volume fraction profiles of the solid phase, in the initial period of settling, is shown in Fig. 4. The three distinct layers are clearly formed. The top of the tank is occupied by pure clear liquid and the sludge layer fills the bottom. Between these two layers, there is a suspension layer, in which the solid volume fraction remains essentially constant and equal to

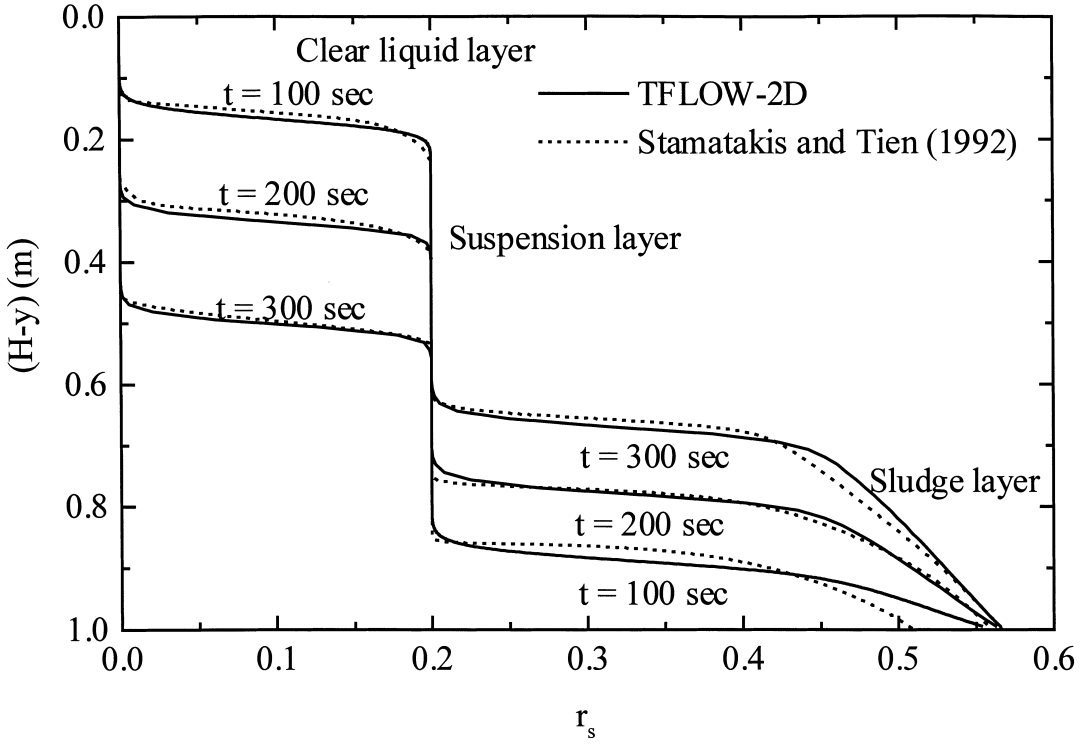

Fig. 4. Solid particle volume fraction distribution at different times.

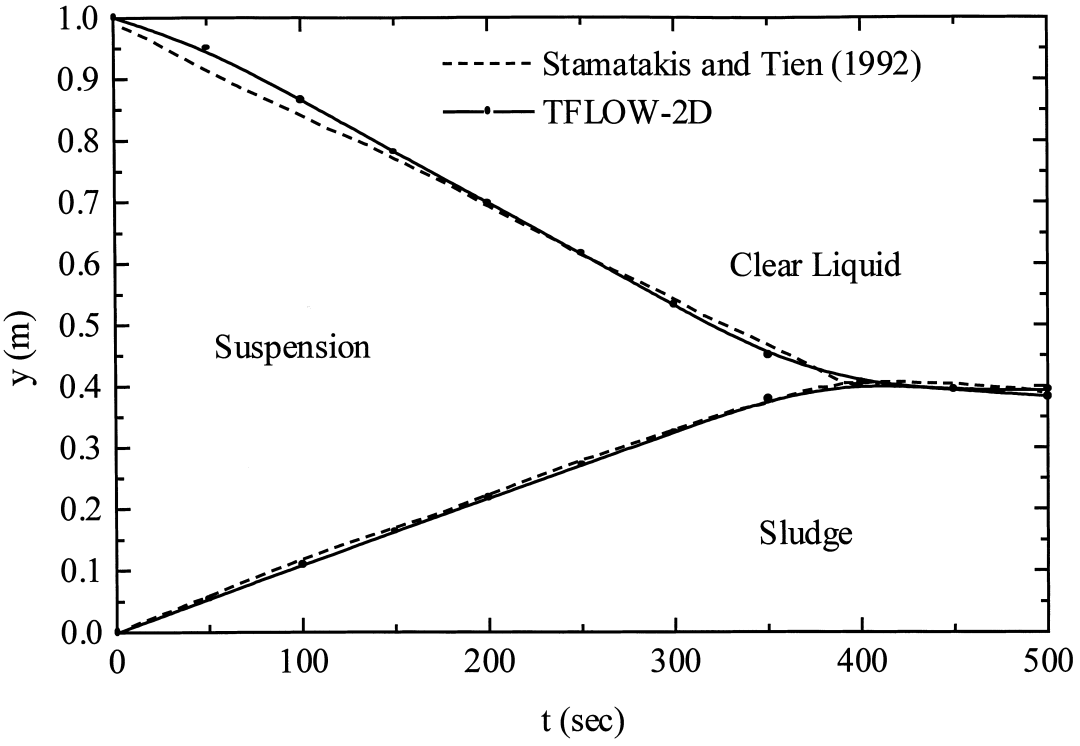

Fig. 5. Progress of sludge-suspension and clear-liquid-suspension interfaces.

the initial value of the solids volume fraction ($r_S = 0.2$). Model calculations are in good agreement with the results of the model predictions of Stamatakis and Tien [5].

Fig. 5 portrays the locations of the two interfaces, i.e. the clear liquid-suspension and the suspension-sludge interfaces, as a functions of time. During the process of sedimentation, which starts at $t = 0$ and ends at $t = 400$ s, the sludge layer thickness increases with time until all particles from the suspension enter the sludge layer. After $t = 400$ s, the thickness of the sludge layer decreases, due to thickening and asymptotically approaches a constant value, which is approximately equal to 0.35 m. The variation of the thickness of the sludge layer with time is also presented in Fig. 6.

3.3. 1-D batch sedimentation of mono-dispersed suspension – comparison with experiments of Hanumanth et al. [9]

Silicon carbide particles settle into liquid aluminium with densities of $\rho_{SiC} = 3200$ kg/m^3 and $\rho_{Al} = 2400$ kg/m^3, respectively. The diameter of the particles is 90 μm, the tank's height 0.25 m and the tank's diameter 0.3 m. The interface friction factor is calculated by Eq. (6). Simulations were made for initial particle volume fractions of 0.05, 0.10, 0.15, 0.20 and 0.30. The results are shown in Fig. 7. The simulations agree with the experimental values of Hanumanth et al. [9].

3.4. 2-D batch sedimentation in tanks with inclined walls

The batch sedimentation calculations of the previous case presented in Section 3.2 have been repeated for the same input data for a settling tank having inclined walls. The 2-D

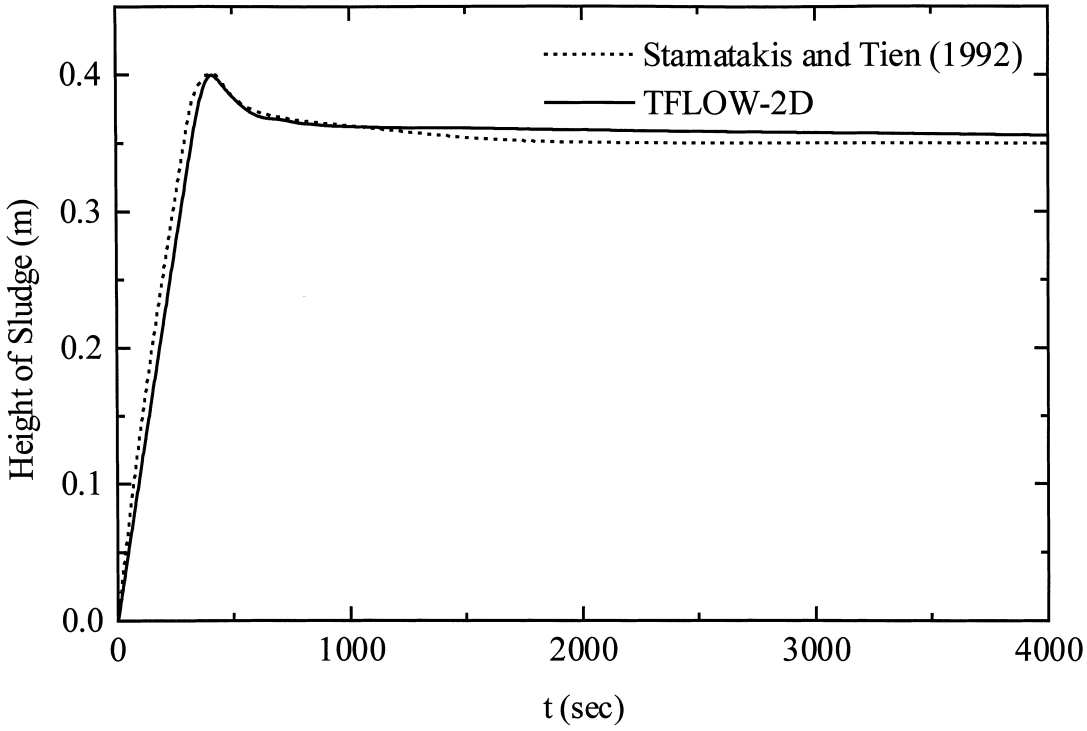

Fig. 6. Sludge height.

version of the model has been used to demonstrate the capability of the present approach to depict the time history of the process by calculating the two velocity components and the volume fraction profiles. In the calculations the effect of the inclination angle, θ, is studied.

In Fig. 8 the velocity vectors of the sludge and the clear liquid at $t = 300$ s are shown for inclination angles $\theta = 30°, 45°$, and $60°$ to the vertical axis. The corresponding volume fractions of the sludge and clear liquid as functions of time are shown in Fig. 9 for inclination angles $\theta = 0°, 30°, 45°$, and $60°$. The model predictions of Figs. 8 and 9 are in a very good qualitative agreement with the findings of Kapoor and Acrivos [16], who suggested that there are five different regions of the flow field in a typical 2-D inclined settler. Unfortunately, a quantitative comparison with Kapoor and Acrivos' data [16] was not possible, due to the lack of information for the geometry of the tanks and the flowrates. Region A (Fig. 9) depicts the clear fluid liquid reservoir, which is characterised by low liquid velocities (Fig. 8). Region B is the liquid layer formed underneath the downward facing surface, which, under the action of buoyancy, is convected rapidly towards the top of the vessel into region A. As shown in Fig. 8, region B is characterised by high clear fluid velocities, parallel to the wall, with magnitudes, which increase with θ. The interface region C separates the clear fluid layer from the adjoining suspension region D, within which the particle volume fraction remains constant through the sedimentation process. Regions B, C and D are clearly indicated in Figs. 8 and 9, and concentration zones of the same particle volume fraction are depicted. In regions A, B, C and D, the pure liquid velocity vectors show a massive recirculation region occupying the whole area, while the velocity vectors of the sludge are generally uni-directional parallel to the vertical walls. However, as θ increases, the liquid velocity vectors show an upward movement in region B, i.e. underneath the downward

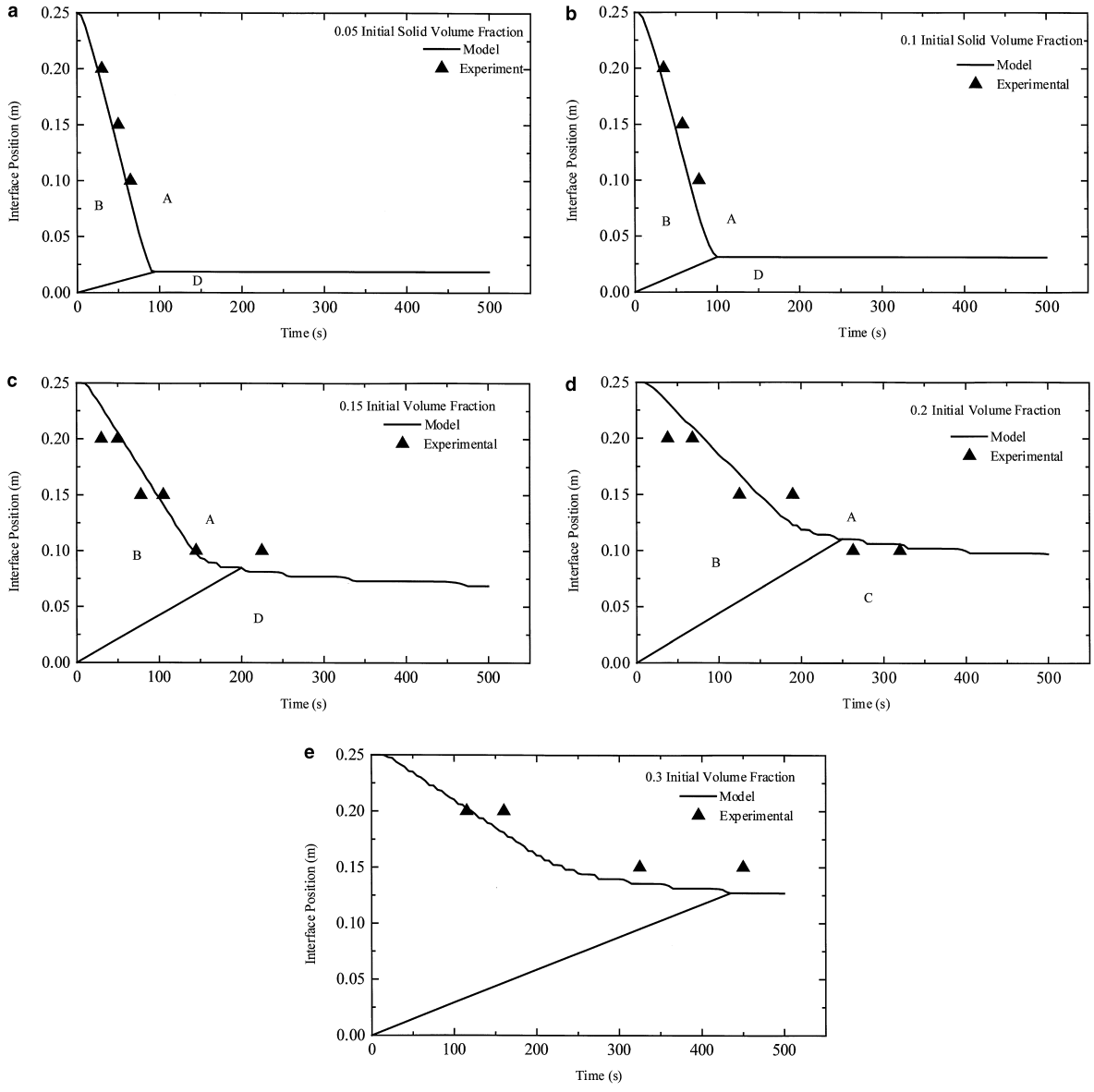

Fig. 7. Progress of clear liquid-suspension interface – comparison with experimental results [9].

facing surface, indicating that in this region the particles are carried away by the strong clear fluid current. In region E the solids are deposited with very low velocities, flowing down the inclined side of the tank. This downward sludge flow is accompanied by an upward flow of the clear liquid with very low velocities, as shown in Fig. 8.

In Fig. 10 the variation of the clear liquid–suspension interface with time, for various inclination angles is shown. As expected, the sedimentation rate increases with θ. When the sedimentation period is over, thickening starts and the interface line becomes almost horizontal. Practically, Fig. 10 suggests that the use of large values of θ increases the sedimentation rate. This is valid only within certain limits of θ, which in real tube settlers are dictated by flow stability criteria [17].

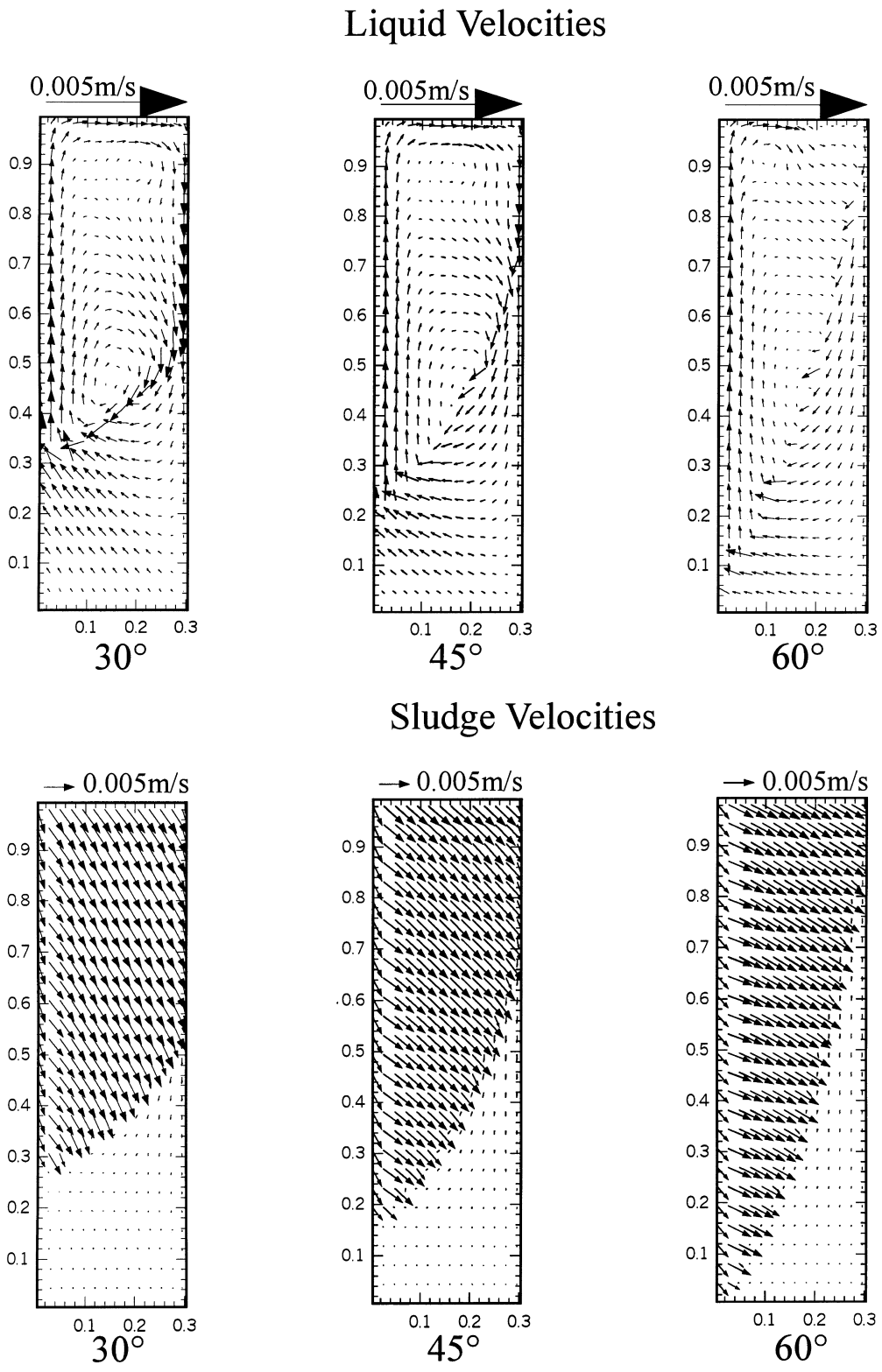

Fig. 8. Velocity vectors at time $t = 300$ s.

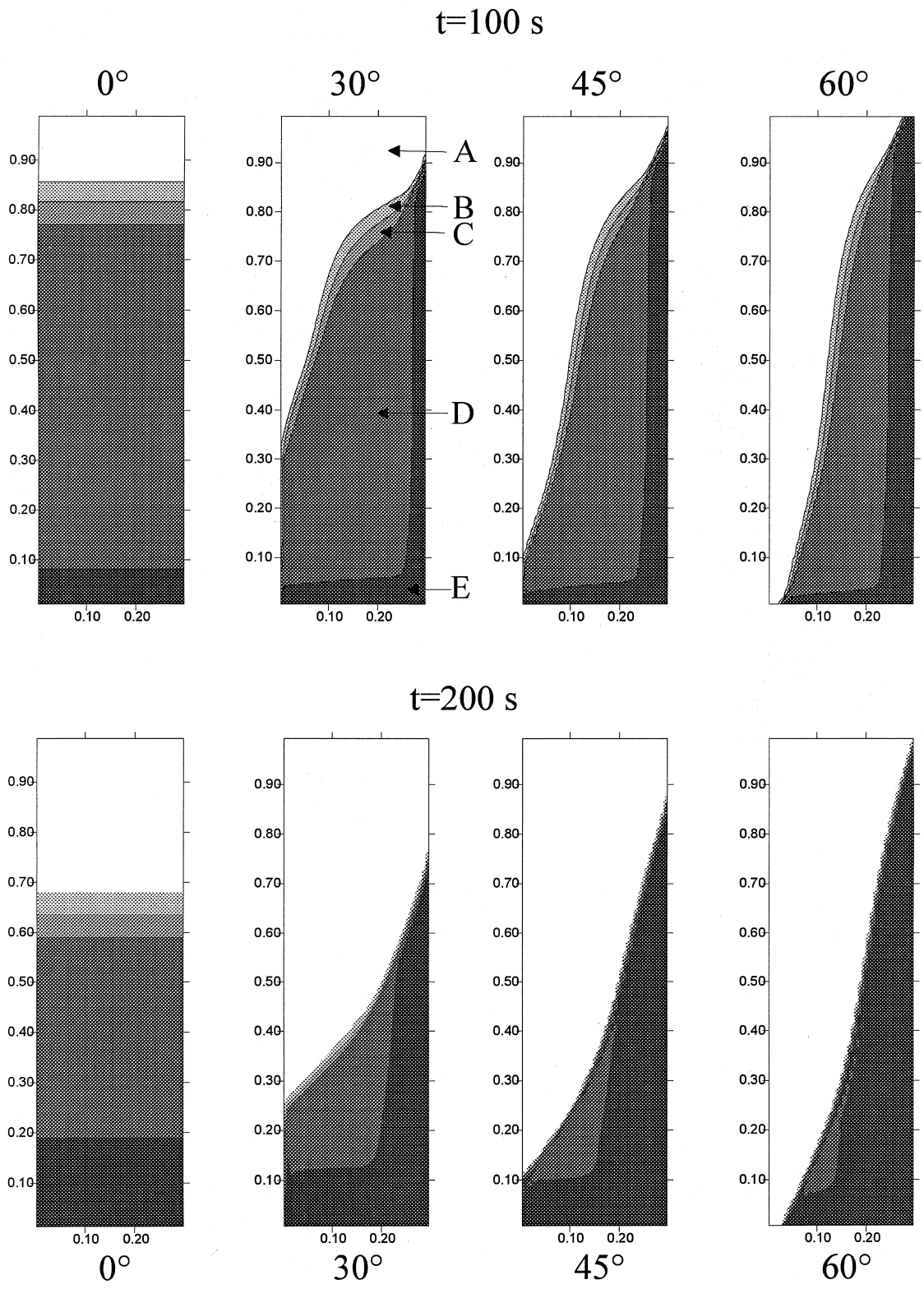

Fig. 9. Particle volume fractions.

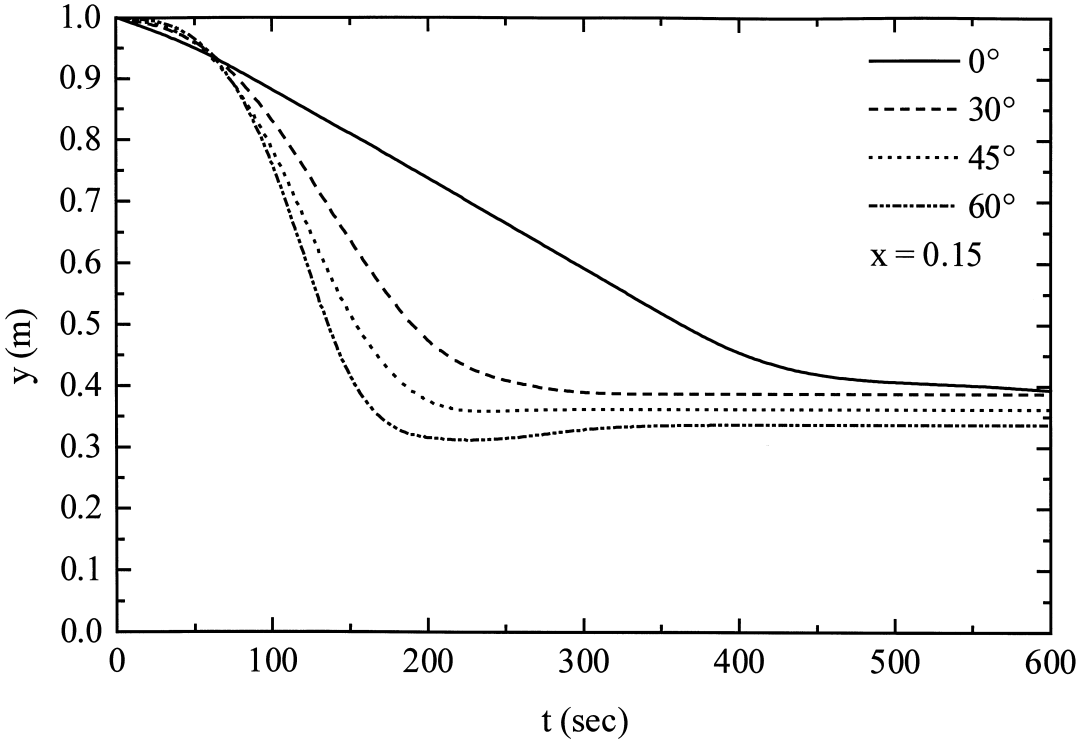

Fig. 10. Clear-liquid–suspension interface at $x = 0.15$ m.

4. Conclusions

This present work sets up an approach to the modeling of sedimentation processes with the following distinctive features:

- The consideration of two-phases, the sludge and the clear fluid.
- The solution of the continuity and momentum equations.
- The interaction between the two phases, which is modeled through the interface friction force and the mixture viscosity.

The model was validated against an analytical solution, numerical predictions of other researchers and experimental data. It predicted well the 1-D sedimentation of a monodispersed suspension and the position of the sludge, suspension and clear liquid zones were in agreement with experimental results.

The extension of the model to two dimensions was also verified qualitatively. The position of the zones of different solid-concentrations was in qualitative agreement with experimental observations. The inclination angle of the settler affected the formation of the zones and it was observed, that the zones of the initial sludge concentration disappear with the increase of the inclination angle, while the clear liquid and sludge zones occupy the largest part of the tank. An increase of the inclination angle accelerates the sedimentation process and produces more clear liquid than smaller inclination angles at the same time period. Although other researchers verify this conclusion, it does not fully reflect the reality, because other phenomena, such as blocking of the settler, prevent the sedimentation process and need to be seriously considered in a further research work.

Appendix A

The continuity, Eq. (A.1), and momentum, Eq. (A.2), equations are:

$$\begin{aligned}
&\frac{\partial}{\partial t}(\rho_1 r_1) + \frac{\partial}{\partial y}(\rho_1 r_1 v_1) = 0,\\
&\frac{\partial}{\partial t}(\rho_2 r_2) + \frac{\partial}{\partial y}(\rho_2 r_2 v_2) = 0,
\end{aligned} \tag{A.1}$$

$$\begin{aligned}
&\frac{\partial}{\partial t}(\rho_1 r_1 v_1) + \frac{\partial}{\partial y}(\rho_1 r_1 v_1 v_1) = -r_1 \frac{\partial P}{\partial y} + C_f r_1 r_2 \bar{\rho}(v_2 - v_1) - \rho_1 r_1 g \cos\theta,\\
&\frac{\partial}{\partial t}(\rho_2 r_2 v_2) + \frac{\partial}{\partial y}(\rho_2 r_2 v_2 v_2) = -r_2 \frac{\partial P}{\partial y} + C_f r_2 r_1 \bar{\rho}(v_1 - v_2) - \rho_2 r_2 g \cos\theta.
\end{aligned} \tag{A.2}$$

Zero divergence is assumed

$$\frac{\partial \bar{v}}{\partial x} = 0, \tag{A.3}$$

which means

$$\bar{v} = r_1 v_1 + r_2 v_2 = 0. \tag{A.4}$$

Combining the continuity and momentum equations, and assuming that the velocities of both phases are almost similar:

$$\begin{aligned}
&r_1 \rho_1 \left(\frac{\partial v_1}{\partial t} + v_1 \frac{\partial v_1}{\partial y} \right) = -r_1 \frac{\partial P}{\partial y} + C_f \bar{\rho} r_1 r_2 (v_2 - v_1) + r_1 \rho_1 g,\\
&r_2 \rho_2 \left(\frac{\partial v_2}{\partial t} + v_2 \frac{\partial v_2}{\partial y} \right) = -r_2 \frac{\partial P}{\partial y} + C_f \bar{\rho} r_1 r_2 (v_1 - v_2) + r_2 \rho_2 g.
\end{aligned} \tag{A.5}$$

Eliminating the pressure gradient

$$\rho_1 \left(\frac{\partial v_1}{\partial t} + v_1 \frac{\partial v_1}{\partial y} \right) - \rho_1 \left(\frac{\partial v_2}{\partial t} + v_2 \frac{\partial v_2}{\partial y} \right) = (\rho_1 - \rho_2) g - C_f \bar{\rho}(v_1 - v_2). \tag{A.6}$$

Assuming great values of the interface friction terms, the accelerating terms in Eq. (A.6) (left part) can be ignored. Therefore the relative velocity of the two phases is

$$V = v_1 - v_2 = \frac{(\rho_1 - \rho_2) g}{C_f \bar{\rho}}. \tag{A.7}$$

When the densities are almost similar and because $\bar{\rho} = 0.5(\rho_1 + \rho_2)$, it is $v_1 = (1 - r_1)V$. Replacing v_1 in the momentum equation:

$$\frac{\partial r_1}{\partial t} + (1 - 2r_1) V \frac{\partial r_1}{\partial y} = 0. \tag{A.8}$$

Dividing the terms of (17) with V

$$\frac{\partial r_1}{\partial \tau} + (1 - 2r_1) \frac{\partial r_1}{\partial y} = 0, \tag{A.9}$$

where $\tau = Vt$.

Eq. (A.9) is a Burger equation, and therefore it can be solved with the method of characteristics. Finally [13]:

$$
\begin{aligned}
&0<\tau<D, \quad r_1=\begin{cases}1, & -D<y<-\tau,\\ 0.5(1-y/\tau), & -\tau<y<\tau,\\ 0, & \tau<y<D,\end{cases}\\
&D<\tau<4D, \quad r_1=\begin{cases}0, & -D<y<-H,\\ 0.5(1-y/\tau), & -H<y<H,\\ 1, & H<y<D,\end{cases}\\
&H=2\sqrt{D\tau}-\tau, \quad \tau\geqslant 4D, \qquad r_1=\begin{cases}0, & y<0,\\ 1, & y>0.\end{cases}
\end{aligned}
\tag{A.10}
$$

In this particular case the ys values are between $[-L/2, L/2]$, thus $D = L/2$. Hence the dense phase settles after a time period of $\tau = 4D$.

The above solution is valid only when the relative velocity of the phases V, is a function of time and position (y). The variable τ is equal to $\tau = \int V\,\mathrm{d}t$. Assuming V independent of y, the volume fractions vary linearly with y

$$
\frac{\partial r_1}{\partial y}=-\frac{\partial r_2}{\partial y}=-\frac{1}{2\tau}. \tag{A.11}
$$

Thus

$$
\begin{aligned}
&\frac{\partial v_1}{\partial t}+v_1\frac{\partial v_1}{\partial y}=\frac{\partial}{\partial t}(r_2V)+r_2V\frac{\partial}{\partial y}(r_2V)=r_2\frac{\mathrm{d}V}{\mathrm{d}t}+\frac{r_1V^2}{2\tau},\\
&\frac{\partial v_2}{\partial t}+v_2\frac{\partial v_2}{\partial y}=\frac{\partial}{\partial t}(r_1V)+r_1V\frac{\partial}{\partial y}(r_1V)=-r_1\frac{\mathrm{d}V}{\mathrm{d}t}+\frac{r_1V^2}{2\tau}.
\end{aligned}
\tag{A.12}
$$

By replacing the second equation of Eq. (A.5)

$$
(r_2\rho_1+r_1\rho_2)\frac{\mathrm{d}V}{\mathrm{d}t}+\bar{\rho}\frac{V^2}{2\tau}=(\rho_1-\rho_2)g-C_\mathrm{f}\bar{\rho}V. \tag{A.13}
$$

Because the density differences are small, it is then $\hat{\rho} = r_2\rho_1 + r_1\rho_2 \approx \bar{\rho}$, and by substituting $\hat{\rho}$ with $\bar{\rho}$, the equation becomes:

$$
\frac{\mathrm{d}V}{\mathrm{d}t}+\frac{V^2}{2\tau}=\frac{(\rho_1-\rho_2)}{\bar{\rho}}g-C_\mathrm{f}V, \quad V=\frac{\mathrm{d}\tau}{\mathrm{d}t}. \tag{A.14}
$$

For great time periods the left part of the equation could be approached by:

$$
\frac{\mathrm{d}V}{\mathrm{d}t}+\frac{V^2}{2\tau}\approx\frac{V^2}{2\tau}=\frac{V^2}{2Vt}=\frac{V^2}{2t},
$$

thus

$$
V=\frac{((\rho_1-\rho_2)/\bar{\rho})gt}{C_\mathrm{f}t+0.5}. \tag{A.15}
$$

Hence

$$
\tau=\int V\,\mathrm{d}t=\frac{(\rho_1-\rho_1)}{\bar{\rho}}g\left(\frac{t}{C_\mathrm{f}}-\frac{\ln(2C_\mathrm{f}t+1)}{2C_\mathrm{f}^2}\right). \tag{A.16}
$$

When the friction factor is equal to zero

$$
\tau=0.25\frac{(\rho_1-\rho_2)}{\bar{\rho}}gt^2. \tag{A.17}
$$

References

[1] G.J. Kynch, Trans. Faraday Soc. 48 (1952) 166.
[2] F.M. Tiller, J. A.I.Ch. E. 27 (1981) 823.
[3] F.M. Auzerais, R. Jackson, W.B. Russel, J. Fluid. Mech. 195 (1988) 437.
[4] K. Stamatakis, T. Chi, Dynamics of batch sedimentation of polydispersed suspensions, Powder Technology 56 (1988) 105–117.
[5] K. Stamatakis, T. Chi, Batch sedimentation calculations – the effect of compressible sediment, Powder Technology 72 (1992) 227–240.
[6] R. Davis, E. Herbolzheimer, A. Acrivos, The Sedimentation of Polydisperse Suspensions Vessels Having Inclined Walls, Internat. J. Multiphase Flow 8 (6) (1982) 571.
[7] H. Wang, R. Davis, Simultaneous sedimentation and coalescence of a dilute dispersion of small drops, J. Fluid Mech. 295 (1995) 247–261.
[8] Bailey et al., Numerical modeling of multiphase particulate flow and its application to sedimentation, Particulate Sci. Technol., 5 (1987) pp. 357–370.
[9] G.S. Hanumanth, G.A. Irons, S. Lafreniere, Particle sedimentation during processing of liquid metal–matrix composites, Metallurgical Trans. B 23 (1992) 753–763.
[10] D.B. Spalding, IPSA 1981; New Developments and Computed Results, CHAM HTS/81/2, 1981.
[11] H.I. Rosten, D.B. Spalding, PHOENICS-84 Reference Handbook, CHAM TR/100, September 17, 1985.
[12] M. Ishii, N. Zuber, Drag coefficient and relative velocity in bubbly, droplet or particulate flows, AlChE J. 25 (5) (1979) 843–855.
[13] D.L. Youngs, Numerical benchmark problem 2a: Sedimentation, International Workshop on two-phase flow fundamentals, 1984.
[14] S.V. Patankar, Numerical heat transfer and fluid flow, McGraw-Hill, New York, 1980.
[15] N.C. Markatos, Mathematical modeling of single- and two-phase flow problems in the process industries, Revue de L Institut Du Petrole vol. 48, no. 6, 1993.
[16] B. Kapoor, A. Acrivos, Sedimentation and sediment flow in settling tanks with inclined walls, J. Fluid Mech. 290 (1995) 39–66.
[17] Leung Woon-Fong, Lamella and tube settlers. 2. Flow Stability, Ind. Eng. Chem. Process Des. Dev. 22 (1983) 68–73.